Enomoto-Iwamoto Motomi (Orcid ID: 0000-0002-1898-5974)
Qin Ling (Orcid ID: 0000-0002-2582-0078)

EGFR signaling is required for maintaining adult cartilage homeostasis and attenuating osteoarthritis progression

Yulong Wei[1,2,a], Xiaoyuan Ma[3,1,a], Hao Sun[1], Tao Gui[1], Jun Li[1], Lutian Yao[1], Leilei Zhong[1], Wei Yu[1,2], Biao Han[4], Charles L. Nelson[1], Lin Han[4], Frank Beier[5], Motomi Enomoto-Iwamoto[6], Jaimo Ahn[1], and Ling Qin[1*]

[1]Department of Orthopaedic Surgery, Perelman School of Medicine, University of Pennsylvania, Philadelphia, Pennsylvania 19104, USA.

[2]Department of Orthopaedics, Union Hospital, Tongji Medical College, Huazhong University of Science and Technology, Wuhan 430022, China.

[3]Department of Orthopaedic Surgery, Qilu Hospital, Cheeloo College of Medicine, Shandong University, Jinan, Shandong 250012, China.

[4]School of Biomedical Engineering, Science and Health Systems, Drexel University, Pennsylvania 19104, USA.

[5]Schulich School of Medicine and Dentistry, University of Western Ontario, London, Ontario N6A 5C1, Canada.

[6]Department of Orthopaedics, School of Medicine, University of Maryland, Baltimore, Maryland 21201, USA

[*] Address correspondence to: Ling Qin, Department of Orthopaedic Surgery, Perelman School of Medicine, University of Pennsylvania, 311A Stemmler Hall, 36th Street and Hamilton Walk, Philadelphia, PA 19104, USA. Tel.: (215) 898-6697; Fax: (215) 573-2133; E-mail: qinling@pennmedicine.upenn.edu

[a] Both authors contributed equally to this work.

Keywords: EGFR, adult cartilage, osteoarthritis, DMM, cartilage degeneration

Running headline: EGFR protects adult cartilage from OA.

Abstract

The uppermost superficial zone of articular cartilage is the first line of defense against the initiation of osteoarthritis (OA). We previously used *Col2-Cre* to demonstrate that EGFR, a tyrosine kinase receptor, plays an essential role in maintaining superficial chondrocytes during articular cartilage development. Here, we showed that EGFR activity in the articular cartilage decreased as mice age. In mouse and human OA samples, EGFR activity was initially reduced at the superficial layer and then resurged in cell clusters within the middle and deep zone in late OA. To investigate the role of EGFR signaling in postnatal and adult cartilage, we constructed an inducible mouse model with cartilage-specific EGFR inactivation (*Aggrecan-CreER* $Egfr^{Wa5/flox}$, *Egfr iCKO*). EdU incorporation revealed that postnatal *Egfr iCKO* mice contained fewer slow-cycling cells than controls. EGFR deficiency induced at 3 months of age reduced cartilage thickness and diminished superficial chondrocytes, in parallel to alterations in lubricin production, cell proliferation and survival. Furthermore, male *Egfr iCKO* mice developed much more severe OA phenotypes, including cartilage erosion, subchondral bone plate thickening, cartilage degeneration at the lateral site, and mechanical allodynia, after receiving destabilization of the medial meniscus (DMM) surgery. Similar OA phenotypes were also observed in female *iCKO* mice. Moreover, Tamoxifen injections of *iCKO* mice at 1 month post surgery accelerated OA development 2 months later. In summary, our data demonstrated that chondrogenic EGFR signaling maintains postnatal slow-cycling cells and plays a critical role in adult cartilage homeostasis and OA progression.

Introduction

Adult articular cartilage is a permanent cartilage with a low turnover rate and a poor healing capacity. In the US, arthritis is a leading cause of disability that affected an estimated 52.5 million (22.7%) adults in 2012 and is expected to affect 78.4 million (25.9%) adults in 2040 [1]. Although osteoarthritis (OA) primarily affects the elderly, sports-related injuries in young population often causes post-traumatic OA. The mainstay treatments for OA are pain management and end stage surgical intervention. The fact that no disease-modifying drugs are available for OA demands more research to understand the signaling regulation of adult articular cartilage.

Cartilage is solely made of chondrocytes and their surrounding extracellular matrix. Growth factors, produced locally or systemically, work in concert to regulate chondrocyte behaviors, such as proliferation, differentiation, matrix production and degradation, survival etc. The most well-studied ones for OA treatment are IGFs, FGFs, TGFβ, BMPs, and PDGFs [2]. Among them, IGF-1 and FGF18 show a plethora of anabolic actions such as promoting chondrocyte proliferation and matrix synthesis without catabolic actions such as matrix degradation. Notably, intra-articular injections of IGF-1 conjugated with cartilage-penetrating nanoparticles are effective in blocking OA development in rats [3]. Further, a phase 2 clinical trial of Sprifermin (rhFGF18) shows promising results in improving joint cartilage thickness of OA patients [4].

Several years ago, our group and others discovered that epidermal growth factor (EGF) family ligands play a critical role in cartilage development, hemostasis, and degeneration via acting on EGF receptor (EGFR) [5]. The mostly expressed EGF family ligands in articular cartilage are TGFα and heparin-binding EGF (HBEGF) [6]. Different from IGF-1 and FGF18, EGF ligands has both anabolic and catabolic actions on primary chondrocytes in culture, which

include stimulating chondrocyte proliferation and survival and their production of lubricant protein [6, 7], inhibiting chondrocyte differentiation and matrix production, and promoting MMP expression [8-10]. In addition, gene profiling studies found that TGFα and HBEGF are up-regulated in OA chondrocytes [9, 11], and high profile genome-wide association studies linked the *TGFA* gene locus to human OA [12-14], suggesting that catabolic effects of this growth factor pathway might prevail over anabolic effects in vivo.

To investigate the role of EGFR signaling in articular cartilage development and OA progression, we previously constructed cartilage-specific EGFR inactivation mice [6]. A dominant negative allele of *Egfr, Wa5* [15], was included to further reduce the remaining EGFR activity due to the low recombination efficiency of *Cre* and *flox* in this model (*Col2-Cre Egfr*$^{flox/Wa5}$). Interestingly, *CKO* articular cartilage exhibited defects in superficial chondrocytes and surface mechanical properties at 2 months of age and developed spontaneous OA at 6 months of age. Applying OA surgery on adult mice causes a more severe OA progression compared to controls. Since *Col2-Cre* targets chondrocytes starting from the embryonic stage, we cannot exclude the possibility that the observed OA phenotypes are secondary to developmental defects. In addition, it cannot dissect the role of EGFR signaling in an OA-stage specific manner. To address this issue, we constructed an inducible chondrocyte-specific EGFR inactivation mouse model using *Aggrecan-CreER* [16]. By administering Tamoxifen at different age groups, we studied the actions of EGFR signaling in postnatal articular cartilage development, adult cartilage homeostasis, and OA degeneration.

Materials and Methods

Study design

This study investigates the role of EGFR signaling in postnatal articular cartilage development, adult cartilage homeostasis, and OA progression. Sample size was determined based on prior experience and indicated in figure legends. In vivo studies used littermates with different genotypes. Animals that died or had severe health problems were excluded. Samples were assigned randomly (coin tossing) to experimental and control groups. The conduct of in vivo experiments was not blinded to the study personnel. In vitro experiments and histological analysis of mouse samples were performed in a blinded fashion.

Animals

All animal work performed in this report was approved by the Institutional Animal Care and Use Committee (IACUC) at the University of Pennsylvania. *Aggrecan-CreER* mice (Jackson Laboratory, Bar Harbor, ME, USA) were bred with $Egfr^{Wa5/+}$ [15] to obtain *Aggrecan-CreER* $Egfr^{Wa5/+}$, which were then crossed with $Egfr^{flox/flox}$ [17] to generate *Aggrecan-CreER* $Egfr^{Wa5/flox}$ *(Egfr iCKO)* mice and their *Wa5* ($Egfr^{Wa5/flox}$) and *WT (Aggrecan-CreER* $Egfr^{flox/+}$ and $Egfr^{flox/+}$*)* siblings. $Egfr^{flox/+}$ mice from the above breeding were used as *WT* for analyzing EGFR signaling components in aging and OA development experiments. Male mice were used in all experiments except otherwise specified. For EdU incorporation study, pups (male and female) received Tamoxifen (50 mg/kg/day) at P1 and P2 followed by intraperitoneal injections of EdU (2.5 mg/kg) at P3-6. Knees were harvested on P7 and P28 for histology analysis. To induce OA, 3-month-old mice received Tamoxifen (75 mg/kg/day) for 5 days followed by destabilization of the medial meniscus (DMM) surgery at right knees and sham surgery at left knees as described previously [18].

Micro-computed tomography (microCT) analysis

Mouse distal femur was scanned at a 6-μm isotropic voxel size with a microCT 35 scanner (Scanco Medical AG, Brüttisellen, Switzerland). All images were smoothened by a Gaussian filter (sigma=1.2, support=2.0). After thresholded corresponding to 472.1 mg HA/cm^3, sagittal images were contoured for subchondral trabecular bone (STB) to quantify bone structural parameters and for subchondral bone plate (SBP) to measure its thickness, as we previously described [19].

Histology

Human cartilage samples were prepared from the de-identified specimens obtained at the total arthroplasty of the knee joints. They were used for histological and immunohistochemical examination.

Mouse knee joints were fixed in 4% paraformaldehyde overnight followed by decalcification in 0.5 M EDTA (pH 7.4) for 4 weeks prior to paraffin embedding. A serial of 6 μm-thick sagittal sections (about 100) were cut across the entire medial compartment of the joint until ACL junction. To measure the thicknesses of articular cartilage and chondrocyte numbers, 3 sections from each knee, corresponding to 1/4 (sections 20-30), 2/4 (sections 45-55), and 3/4 (sections 70-80) regions of the entire section set, were stained with Safranin O/Fast green or hematoxylin and eosin (H&E) and quantified using BIOQUANT software. The final measurement is an average of these three sections. We defined uncalcified cartilage as the area from articular surface to tide mark and calcified cartilage as the area from tide mark to cement line (Fig. S1). Within the uncalcified cartilage area, we counted flat cells at the cartilage surface as superficial chondrocytes and the rest area as transitional and middle zones (TZ+MZ). A similar approach was used on H&E stained sections to measure synovial inflammation score as defined previously F[20]. The method to measure OARSI score was described previously [21]. Briefly, two sections

within every consecutive six sections in the entire section set for each knee were stained with Safranin O/Fast green and scored by two blinded observers. Each knee received a single score representing the maximal score of all its sections.

For immunohistochemistry, paraffin sections were incubated with rabbit anti-EGFR (1:100, CST, 4267), rabbit anti p-EGFR (1:200, Abcam, ab40815), rabbit anti-ERK (1:200, CST, 4695), rabbit anti-p-ERK (1:100, CST, 4370), rabbit anti-Ki67 (1:100, Abcam, ab15580), rabbit anti-TGFα (1:200, Abcam, ab9585), rabbit anti-PRG4 (1:100, Abcam, ab28484), rabbit anti-HBEGF (1:100, Novus Biologicals, AF8239) and rabbit anti-Mig6 (1:100, Abcam, ab227944) at 4°C overnight, followed by incubation with biotinylated secondary antibodies and DAB color development. The terminal deoxynucleotidyl transferase dUTP nick end labeling (TUNEL) assay was carried out according to the manufacturer's instructions (Millipore, s7101). For EdU labeling experiment, using a similar approach as described above, 3 representative sections were selected for EdU staining according to the manufacturer's instructions (Invitrogen, C10337).

AFM-nanoindentation.

Freshly dissected femoral condyle cartilage was indented at more than 10 locations by a borosilicate colloidal spherical tip (R=5 μm, nominal spring constant k=7.4 N/m) with maximum indentation depth of ~1 μm at 10 μm/s indentation rate using a Dimension Icon AFM (BrukerNano) in PBS with protease inhibitors. The effective indentation modulus, E_{ind} (MPa), was calculated by fitting the whole loading portion of each indentation force-depth curve using the Hertz model.

Measurement of mechanical allodynia (von Frey assay)

Individual mouse at 1 month after surgery was placed on a wire-mesh platform (Excellent Technology Co.) under a 4×3×7 cm cage to restrict their move. A set of von Frey fibers

(Stoelting Touch Test Sensory Evaluator Kit) were applied to the plantar surface of the hind paw to determine the paw withdrawal threshold force as described previously [22].

Statistics

All data are presented as boxplots with median with interquartile range where whiskers indicate minimum to maximum. Statistical analysis was performed using GraphPad Prism 8 (GraphPad Software, San Diego, CA) to test the significance of independent variables including age, genotype, surgery type and time after surgery. Distribution of each outcome parameter was checked using histograms and Q-Q plots. For normally distributed data, to test the significance of between-group variables such as age, genotype and time after surgery, unpaired t-test for two groups, or one-way ANOVA with Dunnett's or Tukey-Kramer post-hoc test and two-way ANOVA with Tukey-Kramer post-hoc test. To test the significance of within-subject variable such as surgery type (Sham versus DMM), paired two-sample t-test or repeated-measures ANOVA was applied instead. For non-normally distributed data, Kruskal-Wallis test with Bonferroni post-hoc text was applied. $P < 0.05$ was considered statistically significant.

Results

EGFR activity declines during aging and OA development.

To understand the role of EGFR signaling in articular cartilage, we first performed a comprehensive analysis of EGFR signaling components in the articular cartilage of growing, adult, and aging mice. At early postnatal stage (1 week of age, Fig. 1Aa), EGFR, p-EGFR (an indicator of EGFR activity), its ligands TGFα and HBEGF, as well as its endogenous inhibitor Mig6 [23] were ubiquitously expressed in the epiphyseal cartilage of mouse long bones (Fig. 1Ab-f). At adolescent (1 month of age) and adult (4 months of age) stages (Fig. 1Ag,m), while the

expression of EGFR, TGFα, and HBEGF remained throughout the entire articular cartilage (Fig. 1Ah,j,k,n,p,q), p-EGFR was predominantly present at the top layer of cartilage (Fig. 1Ai,o) and Mig6 staining was barely detectable (Fig. 1Al,r). When mice grew old (7 and 13 months of age, Fig. 1As,y), the percentages of chondrocytes positive for EGFR, p-EGFR, TGFα, and HBEGF in uncalcified cartilage drastically decreased (Fig. 1At-w,z-ac, 1B). However, the ratio of p-EGFR and EGFR positive cells did not change (Fig. 1C), suggesting that the decrease of EGFR expression contributes to the reduction of EGFR activity during aging. Mig6 amount remained absent in aging cartilage (Fig. 1Ax,ad). These data indicate that EGFR activity is negatively correlated with aging.

The change in EGFR activity during OA progression was also examined. DMM surgery induces OA-like phenotypes in mouse knees with a slow progression [24]. Interestingly, DMM did not alter EGFR amount but greatly reduced p-EGFR, TGFα, and HBEGF amounts and elevated Mig6 amount at 1 month post surgery (Fig. 2A, B), suggesting that EGFR activity is reduced when OA initiates.

Human cartilage samples allowed us to study these pathway components at various OA stages (Fig. 2Ca,g,m,s). While strong EGFR staining was always observed throughout the cartilage (Fig. 2Cb,h,n,t, D), p-EGFR was mostly detected in the superficial zone (SZ) and transitional zone (TZ) of normal cartilage (Fig. 2Cc). When OA initiates, p-EGFR was remarkably reduced (Fig. 2Ci,o, D). At late OA stage when SZ and TZ are depleted, p-EGFR staining recurred in clustered chondrocytes under the damaged surface (Fig. 2Cu). TGFα and HBEGF shared the same expression pattern as p-EGFR except that their recurrence starts from middle OA (Fig. 2Cd,e,j,k,p,q,v,w, D). Mig6 staining was almost undetectable in normal cartilage, elevated after OA initiates, and maintained at a high level at middle and late OA stages

(Fig. 2Cf,l,r,x, D). In summary, both human and mouse data demonstrated a loss of EGFR signaling during OA initiation, possibly due to reduced expression of EGFR ligands and enhanced expression of EGFR inhibitor Mig6 after injury.

EGFR activity maintains slow-cycling cells during development.

Recent studies using long-term EdU labeling and lineage tracing approaches have identified slow-cycling cells responsible for forming articular cartilage within the SZ of knee [25, 26] and temporomandibular joints [27]. To eliminate the effect of EGFR signaling on fetal cartilage tissue, we constructed inducible cartilage-specific EGFR knockout mice, *Aggrecan-CreER* $Egfr^{flox/Wa5}$ (*Egfr iCKO*) mice, as well as their *Wa5* and *WT* controls. Our previous studies indicated that *Wa5*, a dominant negative allele of *Egfr*, is required for maximally reduction of EGFR activity in vivo. Pups received Tamoxifen at P1-2 and EdU at P3-P6 daily (Fig. 3A). Tamoxifen injections effectively reduced p-EGFR amount in *iCKO* cartilage compared to *WT* and *Wa5* (Fig. 3Ba-c). Note that *Egfr iCKO* mice express Wa5, a single amino acid mutant of EGFR. Therefore, total EGFR remained at the same level among 3 groups (Fig. 3Bd-f). Quantification confirmed a significant reduction in the ratio of p-EGFR/EGFR positive cells in the articular cartilage of *iCKO* mice compared to *WT* and *Wa5* mice (Fig. 3C).

At P7, the periarticular layer of epiphyseal cartilage, which later becomes articular cartilage, contained similar percentages of EdU^+ cells among *WT, Wa5*, and *iCKO* mice, indicating that EGFR signaling is not required for neonatal proliferation of periarticular cartilage (Fig. 3Da-c, E). Three weeks later, EdU^+ cells in the articular cartilage were all reduced in 3 groups (Fig. 3Dd-f, E). Interestingly, this reduction was more drastic in *iCKO* mice, suggesting a critical role of EGFR signaling in maintaining slow-cycling cells during articular cartilage development.

EGFR signaling is critical for adult cartilage homeostasis.

Because EGFR activity remains high in the top layer of articular cartilage in adult mice at 4 months of age, we next examined whether EGFR signaling is required for maintaining adult cartilage. To do so, 3-month-old mice received Tamoxifen and their knees were harvested at 1 and 3 months later (Fig. 4A). The amounts of EGFR activity indicators, p-EGFR and p-ERK, were significantly decreased in the articular cartilage of *iCKO* mice at 4 months of age (Fig. 4B, C). Meanwhile, we observed a reduced articular cartilage thickness in *Wa5* mice compared to *WT* (Fig. 4Da,b, E) but no difference between *Wa5* and *iCKO* mice (Fig. 4Dc, E). Two months later, while *WT* and *Wa5* cartilage did not show any change during this period, *iCKO* cartilage, particularly the uncalcified layer, was significantly declined in thickness (Fig. 4Dd-f, E).

To explain this decline in thickness, chondrocyte cellularity was counted. Compared to *WT*, *Wa5* cartilage showed much less superficial chondrocytes at 4 and 6 months of age (Fig. 5Aa,b,d,e, B). While they had similar cellularity as *Wa5* at 4 months of age, *Egfr iCKO* mice exhibited a further decrease of superficial chondrocytes compared to *Wa5* at 6 months of age (Fig. 5Ac,f, B). No changes were observed in transitional and middle zone and calcified cartilage.

Egfr iCKO cartilage showed much less Ki67 staining and more TUNEL staining in uncalcified area than *WT* and *Wa5* cartilage (Fig. 5Ca-f, D), suggesting that EGFR signaling is required for promoting proliferation and blocking apoptosis in adult cartilage. As a lubricant protein, Prg4 is synthesized by chondrocytes in the top layer of articular cartilage [28]. Strikingly, Prg4 staining was almost diminished in *iCKO* cartilage (Fig. 5Cg-i, D), suggesting that EGFR activity is critical for maintaining lubrication in adult cartilage. Interestingly, *Wa5* mice also displayed a decrease in $Ki67^+$ cells, an increase in $TUNEL^+$ cells, and a decrease in $Prg4^+$ cells, compared to *WT* mice. In addition, histological staining revealed that anabolic protein type II collagen is reduced in *iCKO* articular cartilage, while catabolic proteins (type X collagen,

Mmp13, and Adamts5) are increased (Fig. S2). These molecular alterations explain structural changes and suggest that EGFR activity is required for normal cartilage homeostasis in adult mice.

EGFR activity attenuates OA initiation in male and female mice.

To delineate the role of EGFR activity during OA initiation, we performed DMM surgery on 3-month-old male mouse knees with Tamoxifen injections right before surgery (Fig. 6A). *WT* mice developed modest OA after DMM surgery with OARSI scores of 0.9, 2.8, and 4.3 at 1, 2, and 3 months post surgery, respectively (Fig. 6Ba,d,g, C). Compared to our previous report [6], Tamoxifen injections did not significantly altered their OA progression. Obvious cartilage degeneration started at 2 months post surgery with a loss of proteoglycan, appearance of fission and cleft and erosion of cartilage and progressed to a more severe level at 3 months post surgery. *Wa5* mice displayed a modestly accelerated cartilage phenotype with significant cartilage degeneration occurring at 1 month post DMM (Fig. 6Bb,e,h). Without Tamoxifen injections, cartilage in *Egfr iCKO* mice had similar appearance as *Wa5* (Fig. S3). However, after Tamoxifen administration, it degenerated quicker than *Wa5* with significant differences starting from 2 months (Fig. 6Bc,f, C). At 3 months post surgery, articular cartilage was mostly depleted in *iCKO* mice (Fig. 6Bi, C). These changes were also reflected in the cartilage thickness, with uncalcified cartilage completely eroded at 2 months and calcified cartilage completely eroded at 3 months in *iCKO* mice (Fig. 6D). On the contrary, *WT* and *Wa5* mice still maintained most of calcified cartilage.

We previously discovered that mechanical changes measured at the microscopic level by nanoindentation is a sensitive indicator of the early onset of OA [29]. In sham legs at 1 month after Tamoxifen injections, *iCKO* femoral cartilage surface showed a significant decrease in E_{ind}

compared to *WT* and *Wa5* (Fig. 6E), suggesting that EGFR is required to maintain mechanical strength in adult cartilage. In both *WT* and *Wa5* knees, DMM injury remarkably decreased E_{ind} at 1 month post surgery, confirming that E_{ind} as a reliable outcome of OA initiation. However, at this stage, *iCKO* cartilage surface showed a drastic increase of E_{ind}, suggesting that it already reaches the late stage of OA when calcified cartilage is exposed.

Subchondral bone sclerosis is a hallmark of late OA [30]. Using a novel CT approach we developed [19], we found that the DMM medial site of SBP underneath OA-damaged cartilage in *iCKO* mice, but not in *WT* or *Wa5*, has significantly elevated thickness compared to other sites (sham medial, sham lateral, and DMM lateral) that are not directly affected by DMM (Fig. 7A, B). Meanwhile, no difference in STB structure or synovitis was observed among 3 groups after DMM (Fig. S4, S5). OA at the medial site eventually leads to cartilage degeneration at the lateral site. Only *iCKO* mice developed modest OA at the lateral site at 3 months post DMM (Fig. 7C, D). In addition, DMM legs in *iCKO* mice displayed much lower paw withdraw threshold toward fiber stimulation compared to *WT* and *Wa5* legs (Fig. 7E), indicating escalated joint mechanical allodynia.

Early study showed that female mice are less susceptible to OA after DMM [31]. We found that *WT* females still develop OA after DMM but the severity is much less than males (Fig. S6Aa,d, B). In line with male data, *Egfr iCKO* females had more severe joint phenotypes, such as complete cartilage depletion and SBP sclerosis, than *Wa5* and *WT* (Fig. S6), demonstrating that EGFR signaling has a cartilage protective role regardless of sex.

EGFR signaling is also required for cartilage protection after OA initiates.

To understand the role of EGFR signaling at different OA stages, we performed DMM surgery on 3-month-old male mice first and then inactivated EGFR by Tamoxifen injections 1

month later (Fig. 8A). After another two months, *Egfr iCKO* mice developed more severe cartilage degeneration (Fig. 8B, C) and SBP thickening (Fig. 8D, E) than *WT* and *Wa5* mice, indicating that inactivation of EGFR after OA initiates also accelerates OA progression.

Discussion

Articular cartilage is maintained by balanced anabolic and catabolic actions of growth factors. Past studies on EGFR signaling pathway have demonstrated its dual regulatory actions on chondrocytes, emphasizing the importance of analyzing this pathway in vivo. Our previous reports of EGFR deficiency in chondrocytes using *Col2-Cre* revealed its distinct roles in growth plate development and articular cartilage development [6, 10, 32] but did not address its specific function in adult cartilage tissues. In this report, using an inducible, cartilage-specific *Aggrecan-CreER* system, we demonstrate that EGFR pathway is essential for maintaining adult articular cartilage homeostasis and preventing cartilage degeneration under OA insults. These actions are achieved by preserving the top layer of articular cartilage, including promoting proliferation, survival, and lubricant production of superficial chondrocytes, and maintaining the mechanical strength of cartilage surface. Results from this study are also complementary to another study from our group showing that chondrocyte-specific overexpression of an EGFR ligand, HBEGF, in adult mice expands the articular cartilage and attenuates OA progression after DMM surgery [33]. Taken together, our data clearly demonstrate that EGFR signaling, activated by EGF family growth factors, predominantly plays a protective role in articular cartilage throughout the life.

Our results are consistent with a recent publication analyzing mice overexpressing *Mig6* in a chondrocyte-specific manner using *Col2-Cre* [34]. In these mice with reduced chondrogenic EGFR activity, articular cartilage appeared normal at 11 weeks of age but developed spontaneous OA at

12 months of age. Mice with cartilage-specific (*Col2-Cre*) or skeleton-specific (*Prrx1-Cre*) deletion of *Mig6*, which have enhanced EGFR activity, showed opposite phenotypes, such as thickened articular cartilage and increased proliferation of superficial layer chondrocytes [35-37]. Mig6 is an endogenous EGFR inhibitor that binds to an extended surface of catalytic domain in ligand-activated EGFR, locks it in an inactive configuration, and targets it for degradation [23]. Our staining revealed that Mig6 level is low in normal adult articular cartilage but is greatly increased after OA initiates. The combination of increased Mig6 amount and decreased TGFα and HBEGF amounts accounts for the reduced EGFR activity at early OA stage.

In human OA samples, while EGFR activity decreases in the articular cartilage at early OA stages, it rebounds at middle and late OA stages when the superficial layer is depleted. Staining for p-EGFR and ligands appeared in clustered chondrocytes under the damaged surface and progressively intensified. This observation correlates well with the previous reports that the amounts of TGFα [7] and HBEGF [9] are increased in human OA samples. In those reports, these results were used as evidence to support a catabolic action of EGFR signaling in cartilage. However, our staining patterns provide an alternative explanation. Increased number and size of cell cluster are a hallmark histologic feature of OA articular cartilage [38]. The cluster formation, primarily through proliferation, is the first response toward cartilage repair after injuries. Interestingly, clusters adjacent to sites of cartilage degeneration have characteristics of progenitor cells with proliferative potential [39]. Thus, the increase of EGFR ligands and the resultant EGFR activity are likely to facilitate cartilage repair by promoting cell proliferation and preventing pre-mature differentiation. Our long-term EdU labeling experiment also uncovered the role of EGFR signaling in maintaining slow-cycling cells in articular cartilage during postnatal development. All these data are consistent with the general role of EGFR signaling in several other tissues,

which is to maintain the stem/progenitor cell pool. Since EGFR is ubiquitously expressed throughout the cartilage, we cannot exclude the additional actions of EGFR on terminally differentiated chondrocytes. Future experiments should be performed to test this possibility.

In mouse knee OA samples, cartilage cell clusters are rarely observed, probably due to the small size of articular cartilage. At 1 month post DMM, articular cartilage shows normal morphology but its mechanical strength has already weakened due to concomitantly elevated proteolytic activities [29]. Meanwhile, we observed that EGFR activity is greatly reduced in DMM joints compared to sham joints. Interestingly, we found that even at this early OA stage with a low EGFR activity, further reduction of EGFR activity in *iCKO* mice leads to accelerated OA progression, indicating that EGFR signaling is critical not only for preventing OA initiation but also for attenuating OA progression. This observation is clinically important in terms of targeting EGFR for OA therapy because OA treatment normally starts after cartilage has already undergone degeneration. Indeed, we previously showed that injections of nanoparticles conjugated with an EGFR ligand, TGFα, in adult mouse knee joints starting from 1 month post DMM prevents further OA progression [33]. Taken together, research from our groups as well as other groups demonstrate that it is suitable to develop clinical applications promoting EGFR signaling for OA treatment.

Traditionally, only males are subjected to DMM surgery as females are less susceptible to it [31]. Recent studies showed that female mice, particular at older ages, also develop OA after DMM, albeit at a much slower pace than males [40]. To mimic clinical OA, we performed DMM surgery on both male and female, skeletally mature animals. We confirmed that OA severity is lessened in *WT* females than *WT* males. Interestingly, OA acceleration is more obvious in *iCKO* females than *iCKO* males because female *WT* mice have a low baseline of OA after DMM surgery.

Hence, we conclude that, when studying accelerated OA phenotypes in the DMM model, female mice are more advantageous than male mice because of increased pathological difference between *WT* and mutant.

In summary, our studies demonstrate that EGFR signaling predominantly plays an anabolic role in postnatal and adult articular cartilage. Upon OA insults, EGFR signaling is required for limiting cartilage degeneration and possibly for regeneration. One limitation of our study is that we cannot study the role of EGFR signaling in late OA stage because first, mouse cartilage layer is quickly eroded after DMM surgery and second, *aggrecan-CreER* activity is low in late OA cartilage. In the future, we will adopt large animal OA models to dissect its role at distinct OA stages. Another limitation is that we only used a specific type of OA mouse model, induced by DMM surgery that causes joint instability. Since OA etiology varies, we should ask the same question in different models, such as non-invasive acute traumatic OA model, chemically-induced ECM degeneration OA model, and aging OA model. The third limitation is that our animal model contains Wa5, an EGFR mutant allele, throughout the development. Therefore, we cannot completely exclude subtle developmental effects on adult cartilage. Nevertheless, studies reported here and previously from our groups and others add EGF-like ligands as another important growth factor family essential for articular cartilage homeostasis and diseases. Future extensive studies are warranted to test its potential as a possible OA therapy.

Acknowledgments

We thank Dr. Waixing Tang in the Histology Core and Drs. Wei-Ju Tseng and Yilu Zhou in the Imaging Core of Penn Center for Musculoskeletal Disorders for technical assistance. We also

thank Dr. Louis Soslowsky and Ms. Stephanie Weiss in the Department of Orthopaedic Surgey, University of Pennsylvania, for providing mouse knee joint sections.

Author Contributions: L.Q. and Y.W. designed the study. Y.W., X.M., H.S., T.G., L.Y., W.Y., and L.Z. performed animal experiments. Y.W., X.M., J.L., H.S., T.G., L.Y., W.Y., and L.Z. performed histology and imaging analysis. B.H. and L.H. performed the nanoindentation experiments. C.N., L.H., F.B., M.E. and J.A. provided administrative, technical, or material support and consultation. L.Q. and Y.W. wrote the manuscript. All authors reviewed and revised the manuscript. L.Q. approved the final version.

Funding Sources

This study was supported by NIH grants R01AG067698 (to L.Q.), R01AR074490 (to L.H.) and P30AR069619 (to Penn Center for Musculoskeletal Disorders).

Conflict of Interest

The authors declare no conflicts of interest.

Data Availability Statement

All data associated with this study are present in the paper and available from the corresponding authors upon reasonable request.

References

1. Barbour KE, Helmick CG, Boring M, Zhang X, Lu H, Holt JB. Prevalence of Doctor-Diagnosed Arthritis at State and County Levels - United States, 2014. MMWR Morb Mortal Wkly Rep 2016; 65: 489-494.
2. Fortier LA, Barker JU, Strauss EJ, McCarrel TM, Cole BJ. The role of growth factors in cartilage repair. Clin Orthop Relat Res. 2011; 469: 2706-2715.
3. Geiger BC, Wang S, Padera RF, Jr., Grodzinsky AJ, Hammond PT. Cartilage-penetrating nanocarriers improve delivery and efficacy of growth factor treatment of osteoarthritis. Sci Transl Med. 2018; 10: eaat8800. .
4. Hochberg MC, Guermazi A, Guehring H, Aydemir A, Wax S, Fleuranceau-Morel P, et al. Effect of Intra-Articular Sprifermin vs Placebo on Femorotibial Joint Cartilage Thickness in Patients With Osteoarthritis: The FORWARD Randomized Clinical Trial. JAMA. 2019; 322: 1360-1370.
5. Qin L, Beier F. EGFR Signaling: Friend or Foe for Cartilage? JBMR Plu 2019; 3: e10177.
6. Jia H, Ma X, Tong W, Doyran B, Sun Z, Wang L, et al. EGFR signaling is critical for maintaining the superficial layer of articular cartilage and preventing osteoarthritis initiation. Proc Natl Acad Sci U S A. 2016; 113: 14360-14365. .
7. Appleton CT, Usmani SE, Bernier SM, Aigner T, Beier F. Transforming growth factor alpha suppression of articular chondrocyte phenotype and Sox9 expression in a rat model of osteoarthritis. Arthritis Rheum. 2007; 56: 3693-3705.
8. Appleton CT, Usmani SE, Mort JS, Beier F. Rho/ROCK and MEK/ERK activation by transforming growth factor-alpha induces articular cartilage degradation. Lab Invest 2010; 90: 20-30.
9. Long DL, Ulici V, Chubinskaya S, Loeser RF. Heparin-binding epidermal growth factor-like growth factor (HB-EGF) is increased in osteoarthritis and regulates chondrocyte catabolic and anabolic activities. Osteoarthritis Cartilage. 2015; 23: 1523-1531.
10. Zhang X, Zhu J, Li Y, Lin T, Siclari VA, Chandra A, et al. Epidermal growth factor receptor (EGFR) signaling regulates epiphyseal cartilage development through beta-catenin-dependent and -independent pathways. J Biol Chem 2013; 288: 32229-32240.
11. Appleton CT, Pitelka V, Henry J, Beier F. Global analyses of gene expression in early experimental osteoarthritis. Arthritis Rheum. 2007; 56: 1854-1868.

12. Castano-Betancourt MC, Evans DS, Ramos YF, Boer CG, Metrustry S, Liu Y, et al. Novel genetic variants for cartilage thickness and hip osteoarthritis. PLoS Genet. 2016; 12: e1006260. .
13. Cui G, Wei R, Liu D, Yang H, Wu J, Fan L, et al. Association of Common Variants in TGFA with Increased Risk of Knee Osteoarthritis Susceptibility. Genet Test Mol Biomarkers. 2017; 21: 586-591.
14. Zengini E, Hatzikotoulas K, Tachmazidou I, Steinberg J, Hartwig FP, Southam L, et al. Genome-wide analyses using UK Biobank data provide insights into the genetic architecture of osteoarthritis. Nat Genet. 2018; 50: 549-558. .
15. Lee D, Cross SH, Strunk KE, Morgan JE, Bailey CL, Jackson IJ, et al. Wa5 is a novel ENU-induced antimorphic allele of the epidermal growth factor receptor. Mamm Genome 2004; 15: 525-536.
16. Henry SP, Jang CW, Deng JM, Zhang Z, Behringer RR, de Crombrugghe B. Generation of aggrecan-CreERT2 knockin mice for inducible Cre activity in adult cartilage. Genesis. 2009; 47: 805-814.
17. Lee TC, Threadgill DW. Generation and validation of mice carrying a conditional allele of the epidermal growth factor receptor. Genesis. 2009; 47: 85-92.
18. Zhang X, Zhu J, Liu F, Li Y, Chandra A, Levin LS, et al. Reduced EGFR signaling enhances cartilage destruction in a mouse osteoarthritis model. Bone Research 2014; 2: 14015.
19. Jia H, Ma X, Wei Y, Tong W, Tower RJ, Chandra A, et al. Reduction in Sclerostin as a mechanism of subchondral bone plate sclerosis in mouse knee joints during late-stage osteoarthritis. Arthritis Rheumatol 2018; 70: 230-241.
20. Krenn V, Morawietz L, Haupl T, Neidel J, Petersen I, Konig A. Grading of chronic synovitis--a histopathological grading system for molecular and diagnostic pathology. Pathol Res Pract 2002; 198: 317-325. .
21. Glasson SS, Chambers MG, Van Den Berg WB, Little CB. The OARSI histopathology initiative - recommendations for histological assessments of osteoarthritis in the mouse. Osteoarthritis Cartilage. 2010; 18: S17-23.
22. Piel MJ, Kroin JS, Im HJ. Assessment of knee joint pain in experimental rodent models of osteoarthritis. Methods Mol Biol. 2015; 1226: 175-181.

23. Zhang X, Pickin KA, Bose R, Jura N, Cole PA, Kuriyan J. Inhibition of the EGF receptor by binding of MIG6 to an activating kinase domain interface. Nature. 2007; 450: 741-744.
24. Glasson SS, Blanchet TJ, Morris EA. The surgical destabilization of the medial meniscus (DMM) model of osteoarthritis in the 129/SvEv mouse. Osteoarthritis Cartilage. 2007; 15: 1061-1069. .
25. Kozhemyakina E, Zhang M, Ionescu A, Ayturk UM, Ono N, Kobayashi A, et al. Identification of a Prg4-expressing articular cartilage progenitor cell population in mice. Arthritis Rheumatol. 2015; 67: 1261-1273.
26. Li L, Newton PT, Bouderlique T, Sejnohova M, Zikmund T, Kozhemyakina E, et al. Superficial cells are self-renewing chondrocyte progenitors, which form the articular cartilage in juvenile mice. FASEB J. 2017; 31: 1067-1084. .
27. Embree MC, Chen M, Pylawka S, Kong D, Iwaoka GM, Kalajzic I, et al. Exploiting endogenous fibrocartilage stem cells to regenerate cartilage and repair joint injury. Nat Commun. 2016; 7: 13073.
28. Becerra J, Andrades JA, Guerado E, Zamora-Navas P, Lopez-Puertas JM, Reddi AH. Articular cartilage: structure and regeneration. Tissue Eng Part B Rev. 2010; 16: 617-627.
29. Doyran B, Tong W, Li Q, Jia H, Zhang X, Chen C, et al. Nanoindentation modulus of murine cartilage: a sensitive indicator of the initiation and progression of post-traumatic osteoarthritis. Osteoarthritis Cartilage. 2017; 25: 108-117. .
30. Kellgren JH, Lawrence JS. Radiological assessment of osteo-arthrosis. Ann Rheum Dis. 1957; 16: 494-502.
31. Ma HL, Blanchet TJ, Peluso D, Hopkins B, Morris EA, Glasson SS. Osteoarthritis severity is sex dependent in a surgical mouse model. Osteoarthritis Cartilage. 2007; 15: 695-700. .
32. Zhang X, Siclari VA, Lan S, Zhu J, Koyama E, Dupuis HL, et al. The critical role of the epidermal growth factor receptor in endochondral ossification. J Bone Miner Res 2011; 26: 2622-2633.
33. Wei Y, Luo L, Gui T, Yu F, Yan L, Yao L, et al. Targeting cartilage EGFR pathway for osteoarthritis treatment. Sci Transl Med. 2021; 13: eabb3946.
34. Bellini M, Pest MA, Miranda-Rodrigues M, Qin L, Jeong JW, Beier F. Overexpression of MIG-6 in the cartilage induces an osteoarthritis-like phenotype in mice. Arthritis Res Ther. 2020; 22: 119.

35. Pest MA, Russell BA, Zhang YW, Jeong JW, Beier F. Disturbed cartilage and joint homeostasis resulting from a loss of mitogen-inducible gene 6 in a mouse model of joint dysfunction. Arthritis Rheumatol. 2014; 66: 2816-2827.
36. Shepard JB, Jeong JW, Maihle NJ, O'Brien S, Dealy CN. Transient anabolic effects accompany epidermal growth factor receptor signal activation in articular cartilage in vivo. Arthritis 2013; 15: R60.
37. Staal B, Williams BO, Beier F, Vande Woude GF, Zhang YW. Cartilage-specific deletion of Mig-6 results in osteoarthritis-like disorder with excessive articular chondrocyte proliferation. Proc Natl Acad Sci U S A 2014; 111: 2590-2595.
38. Lotz MK, Otsuki S, Grogan SP, Sah R, Terkeltaub R, D'Lima D. Cartilage cell clusters. Arthritis Rheum. 2010; 62: 2206-2218. .
39. Hoshiyama Y, Otsuki S, Oda S, Kurokawa Y, Nakajima M, Jotoku T, et al. Chondrocyte clusters adjacent to sites of cartilage degeneration have characteristics of progenitor cells. J Orthop Res. 2015; 33: 548-555.
40. Huang H, Skelly JD, Ayers DC, Song J. Age-dependent Changes in the Articular Cartilage and Subchondral Bone of C57BL/6 Mice after Surgical Destabilization of Medial Meniscus. Sci Rep. 2017; 7: 42294.

Figure legends

Fig 1. EGFR signaling is reduced during aging. A, Immunohistochemistry staining of EGFR, p-EGFR, TGFα, HBEGF, and Mig6 in tibial articular cartilage of 1-week, 1-, 4-, 7-, and 13-month-old male *WT* mice (Scale bar, 200 μm). Safranin O/Fast green staining of *WT* knee joints at different ages are shown at the left panel. **B,** The percentages of $EGFR^+$, p-$EGFR^+$, $TGF\alpha^+$, $HBEGF^+$, and $Mig6^+$ chondrocytes within the articular cartilage were quantified at indicated ages (n = 8 mice/group). **C**, The ratio of p-EGFR positive cells to EGFR positive cells was quantified (n = 8 mice/group). Statistical analysis was performed using one-way ANOVA with Dunnett's post-hoc test.

Fig 2. EGFR signaling is altered during OA development. A, Immunohistochemistry staining of EGFR, p-EGFR, TGFα, HBEGF, and Mig6 in the tibial articular cartilage of male *WT* mice at 1 month post-sham or -DMM surgery (Scale bar, 200 μm). Safranin O/Fast green staining of *WT* sham and DMM knee joints are shown at the left panel. **B,** The percentages of $EGFR^+$, p-$EGFR^+$, $TGF\alpha^+$, $HBEGF^+$, and $Mig6^+$ chondrocytes within the articular cartilage were quantified (n = 8 mice/group). **C,** Safranin O/Fast green staining, EGFR, p-EGFR, TGFα, HBEGF and Mig6 staining of human healthy and OA articular cartilage at early, middle, and late stages (Scale bar, 200 μm). SZ: superficial zone, TZ: transitional zone, MZ: middle zone, CZ: calcified zone. **D,** The percentages of $EGFR^+$, p-$EGFR^+$, $TGF\alpha^+$, $HBEGF^+$, and $Mig6^+$ chondrocytes within the articular cartilage were quantified in normal and OA human cartilage tissues (n = 8 samples/group). Statistical analysis was performed using paired two-tailed t-test for B and one-way ANOVA with Dunnett's post hoc test for D.

Fig 3. EGFR activity maintains slow-cycling cells in postnatal growth. A, The study protocol of slow-cycling experiment. Postnatal pups received 2 Tamoxifen injections at P1 and P2 followed by 4 daily EdU injections from P3-P6. Knee joints were harvested at 1 and 4 weeks of age for analysis. **B,** Immunofluorescence staining of p-EGFR and EGFR in the tibial articular cartilage of 1-month-old *WT*, *Wa5* and *Egfr iCKO* mice after Tamoxifen and EdU injections (Scale bar, 100 μm). Dashed lines outline articular cartilage. **C,** The ratio of p-EGFR positive cells to EGFR positive cells was quantified (n = 4 mice/group). **D,** EdU staining in the knee joints of 1-week- and 1-month-old *WT*, *Wa5* and *iCKO* mice after Tamoxifen and EdU injections (Scale bar, 100 μm). Dashed lines outline periarticular layer (1week of age) and articular cartilage (4 weeks of age) for analysis. **E,** The percentage of EdU^+ chondrocytes was quantified in the tibial periarticular layer (1 week of age) and articular cartilage (4 weeks of age) (n = 5-6 mice/group). Statistical analysis was performed using one-way ANOVA with Tukey-Kramer post-hoc test for C and two-way ANOVA with Tukey-Kramer post-hoc test.

Fig 4. EGFR signaling contributes to cartilage homeostasis in adult mice. A, The study protocol showed that male *WT*, *Wa5* and *iCKO* mice received 5 daily Tamoxifen injections at 3 months of age to inactivate EGFR, followed by knee joint harvest at 4 and 6 months of age. **B,** Immunohistochemistry staining of p-EGFR, EGFR, p-ERK, and ERK in the tibial articular cartilage of 4-month-old *WT*, *Wa5* and *iCKO* mice (Scale bar, 100 μm). **C,** The percentages of p-$EGFR^+$, $EGFR^+$, p-ERK^+, and ERK^+ chondrocytes within tibial articular cartilage were quantified at 4 months of age (n = 8 mice/group). **D,** Safranin O/Fast green staining of *WT*, *Wa5* and *iCKO* knee joints at the medial site at 4 and 6 months of age (Scale bar, 200 μm). low: low magnification image, high: high magnification image of the yellow boxed areas above. **E,**

Average thicknesses of uncalcified (Uncal. Th.), calcified (Cal.Th.), and total (Total.Th.) tibial articular cartilage were quantified (n = 3-5 mice/group). Statistical analysis was performed using one-way ANOVA with Tukey-Kramer post-hoc test for C and two-way ANOVA with Tukey-Kramer post-hoc test for E.

Fig 5. EGFR signaling maintains superficial chondrocytes via promoting lubricin production, cell proliferation and survival in adult cartilage. A, H&E staining in the femoral articular cartilage of male *WT*, *Wa5* and *iCKO* mice at 4 and 6 months of age (Scale bar, 50 μm)**. B,** Chondrocyte cell densities in superficial zone (SZ), transitional and middle zones (TZ+MZ), calcified zone (CZ), and the entire articular cartilage (Total AC) were quantified (n = 6 mice/group). **C,** Ki67, PRG4 and TUNEL staining in the tibial articular cartilage of *WT*, *Wa5,* and *iCKO* mice at 6 months of age (Scale bar, 50 μm). **D,** The percentages of $Ki67^+$, $TUNEL^+$, and $PRG4^+$ cells in the tibial articular cartilage were quantified (n = 8 mice/group). Statistical analysis was performed using two-way ANOVA with Tukey-Kramer post-hoc test for B and one-way ANOVA with Tukey-Kramer post-hoc test for D.

Fig 6. Chondrogenic EGFR deficiency accelerates OA progression in adult male mice. A, The study protocol showed that male *WT*, *Wa5,* and *iCKO* mice received 5 daily tamoxifen injections right before surgery (sham or DMM) at 3 months of age, their knee joints were harvested at 1, 2 and 3 months post-surgery. **B,** Safranin O/Fast green staining of *WT*, *Wa5* and *iCKO* knee joints at the medial site at 1, 2, and 3 months post-DMM (Scale bar, 200 μm). **C,** OA severity was accessed by OARSI Score (n = 5-9 mice/group). **D,** Average thicknesses of uncalcified (Uncal. Th.), calcified (Cal.Th.), and total (Total.Th.) tibial articular cartilage were

quantified at 1, 2 and 3 months post-DMM (n = 3-5). **E,** Surface modulus (E_{ind}) of sham and DMM femoral articular cartilage was measured by nanoindentation at 1 month post-surgery (n = 4-6 mice/group). Statistical analysis was performed using one-way ANOVA with Tukey-Kramer post-hoc test for C and D (comparison was performed among different genotype at each time point) and two-way ANOVA with Tukey-Kramer post-hoc test for E.

Fig 7. *Egfr iCKO* mice develop late OA symptoms after DMM surgery. A, Representative 3-D color maps show SBP thickness in the femurs of *WT*, *Wa5,* and *iCKO* mice at 3 months post-surgery. Color ranges from 0 (blue) to 430 μm (red)). L: lateral femoral condyle, M: medial femoral condyle. **B,** SBP thickness (SBP Th.) at the medial and lateral femoral condyle of sham and DMM knee joints was measured (n = 6-9 mice/group). **C,** Safranin O/Fast green staining of *WT*, *Wa5* and *iCKO* knee joints at the lateral site at 3 months post-DMM (Scale bar, 200 μm). The bottom panel shows the magnified images of cartilage damage site (yellow boxed areas) from the top panel. **D,** OA severity of lateral site was accessed by OARSI Score (n = 4-5 mice/group). **E,** Joint pain was measured by von Frey assay at 1 months post-surgery (n = 5-7 mice/group). PWT: paw withdrawal threshold. Statistical analysis was performed using one-way ANOVA with Tukey-Kramer post-hoc test for B (comparison was performed among different genotype at each site), D and two-way ANOVA with Tukey-Kramer post-hoc test for E.

Fig 8. EGFR signaling is required for protecting cartilage after OA develops. A, The study protocol showed that male *WT*, *Wa5,* and *iCKO* mice received sham or DMM surgery at 3 months of age followed by 5 daily Tamoxifen injections at 4 months of age and their knee joints were harvested at 6 months of age. **B,** Safranin O/Fast green staining of *WT*, *Wa5,* and *iCKO*

knee joints at the medial site at 6 months of age (Scale bar, 200 μm). low: low magnification image, high: high magnification image of the yellow boxed areas above. **C,** OA severity was accessed by OARSI Score (n = 6 mice/group). **D,** Representative 3-D color maps showed subchondral bone plate thickness (SBP Th.) in the femurs of *WT*, *Wa5,* and *iCKO* mice at 6 months of age. Color ranges from 0 (blue) to 340 μm (red). L: lateral femoral condyle, M: medial femoral condyle. **E,** SBP thickness at the medial and lateral femoral condyle of sham and DMM knee joints was measured (n = 3-6 mice/group). Statistical analysis was performed using two-way ANOVA with Tukey-Kramer post-hoc test for C and one-way ANOVA with Tukey-Kramer post-hoc test for E (comparison was performed among different genotype at each site).

Fig S1. A representative H&E image of tibial articular cartilage from 6-month-old *WT* mice shows the positions of cartilage zones. SZ: superficial zone; TZ: transitional zone; MZ: middle zone; CZ: calcified zone. Uncalcified zone includes SZ, TZ, and MZ. (Scale bar, 200 μm).

Fig S2. EGFR deficiency alters anabolic and catabolic proteins in the cartilage. A, Immunotaining of Col II, Col X, Mmp13, and Adamts5 in the tibial articular of *WT, Wa5* and *Egfr iCKO* mice at 3 months post-DMM (Scale bar, 50 μm). **B,** The Col II staining intensity was quantified (n = 4 mice/group). **C**, The percentage of Col X^+, $Mmp13^+$ and $Adamts5^+$ chondrocytes were quantified (n = 4 mice/group). Statistical analysis was performed using one-way ANOVA with Tukey-Kramer post-hoc test.

Fig S3. *Egfr iCKO* mice with no Tamoxifen injections have similar articular cartilage morphology as *Wa5* mice. A, H&E staining of the articular cartilage from male *WT, Wa5* and

Egfr iCKO mice at 3 months of age (Scale bar, 200 μm). **B,** Average thicknesses of the total (Total.Th.) tibial articular cartilage were quantified (n = 4 mice/group). Statistical analysis was performed using one-way ANOVA with Tukey-Kramer post-hoc test.

Fig S4. EGFR deficiency in articular cartilage does not affect the trabecular bone structure in STB at 3 months after DMM. Trabecular bone structural parameters of distal femoral STB of *WT, Wa5* and *Egfr iCKO* mice were quantified. n = 4 mice/group. BMD: bone mineral density, BV/TV: bone volume/tissue volume, Tb.N: trabecular number, Tb.Th: trabecular thickness, Tb.Sp: trabecular separation, SMI: structure model index. Statistical analysis was performed using Kruskal-Wallis test with Bonferroni post-hoc test.

Fig S5. EGFR deficiency in articular cartilage does not affect synovium tissue structure. Representative H&E stained images of synovium of *WT, Wa5* and *Egfr iCKO* mice at 3 months post sham or DMM surgery. Scale bars, 200 μm. n = 3 mice/group.

Fig S6. Chondrogenic EGFR deficiency in adult female mice accelerates OA progression. A, Safranin O/Fast green staining of female *WT*, *Wa5*, and *iCKO* knee joints at the medial site at 3 months post-surgery (Scale bar, 200 μm). Low: low magnification image, high: high magnification image of the yellow boxed areas above. **B,** OA severity was accessed by OARSI Score (n = 5-7 mice/group). **C,** Representative 3-D color maps showed subchondral bone plate thickness (SBP Th.) in the femurs of female *WT*, *Wa5,* and *iCKO* mice at 3 months post-surgery. Color ranges from 0 (blue) to 280 μm (red). L: lateral femoral condyle, M: medial femoral condyle. **D,** SBP thickness at the medial and lateral femoral condyle of female sham and DMM

knee joints was measured (n = 5-8 mice/group). Statistical analysis was performed using two-way ANOVA with Tukey-Kramer post-hoc test for B and one-way ANOVA with Tukey-Kramer post-hoc test for D (comparison was performed among different genotype at each site).

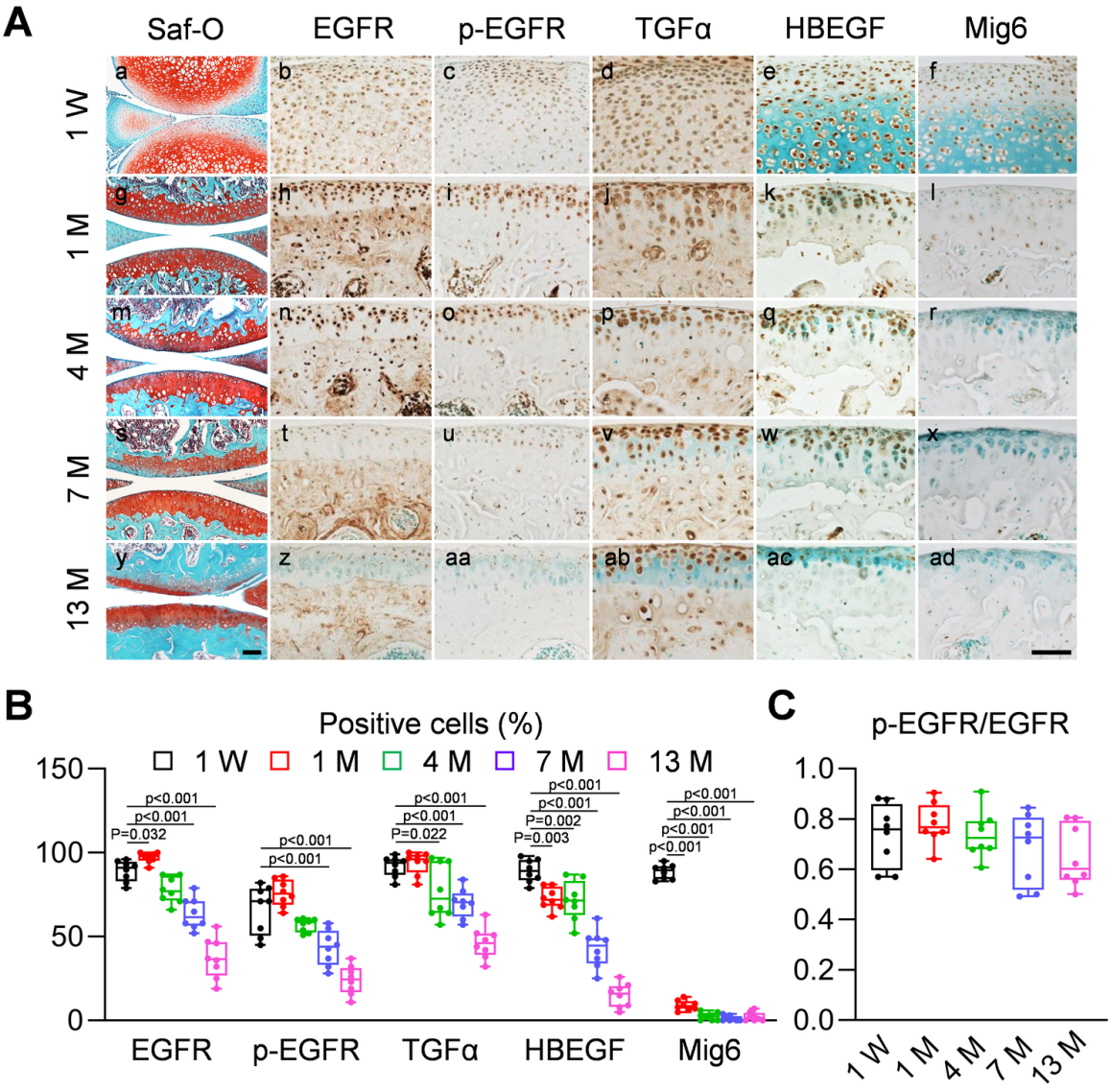

JBMR_4531_Figure 1.tif

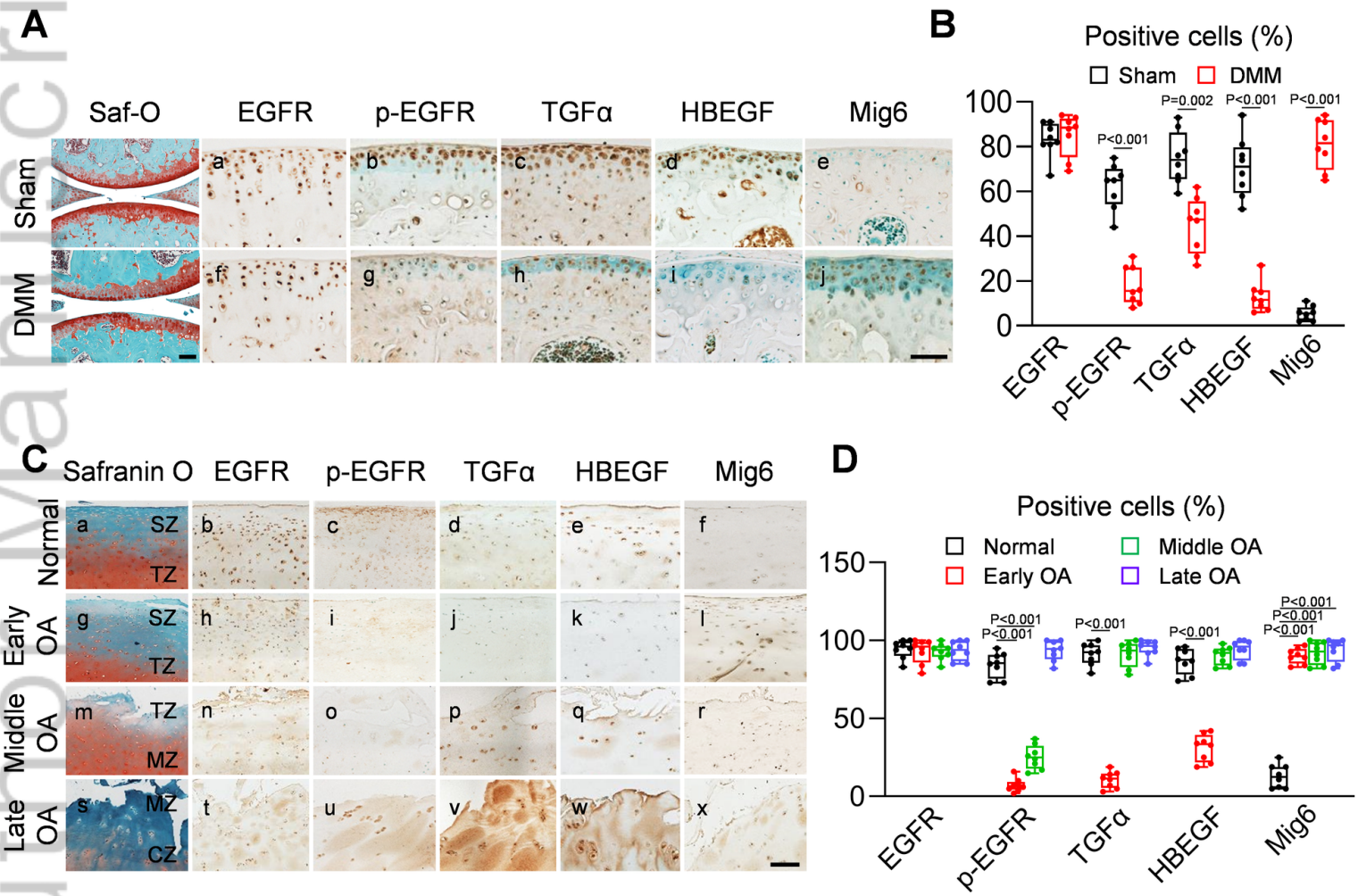

JBMR_4531_Figure 2.tif

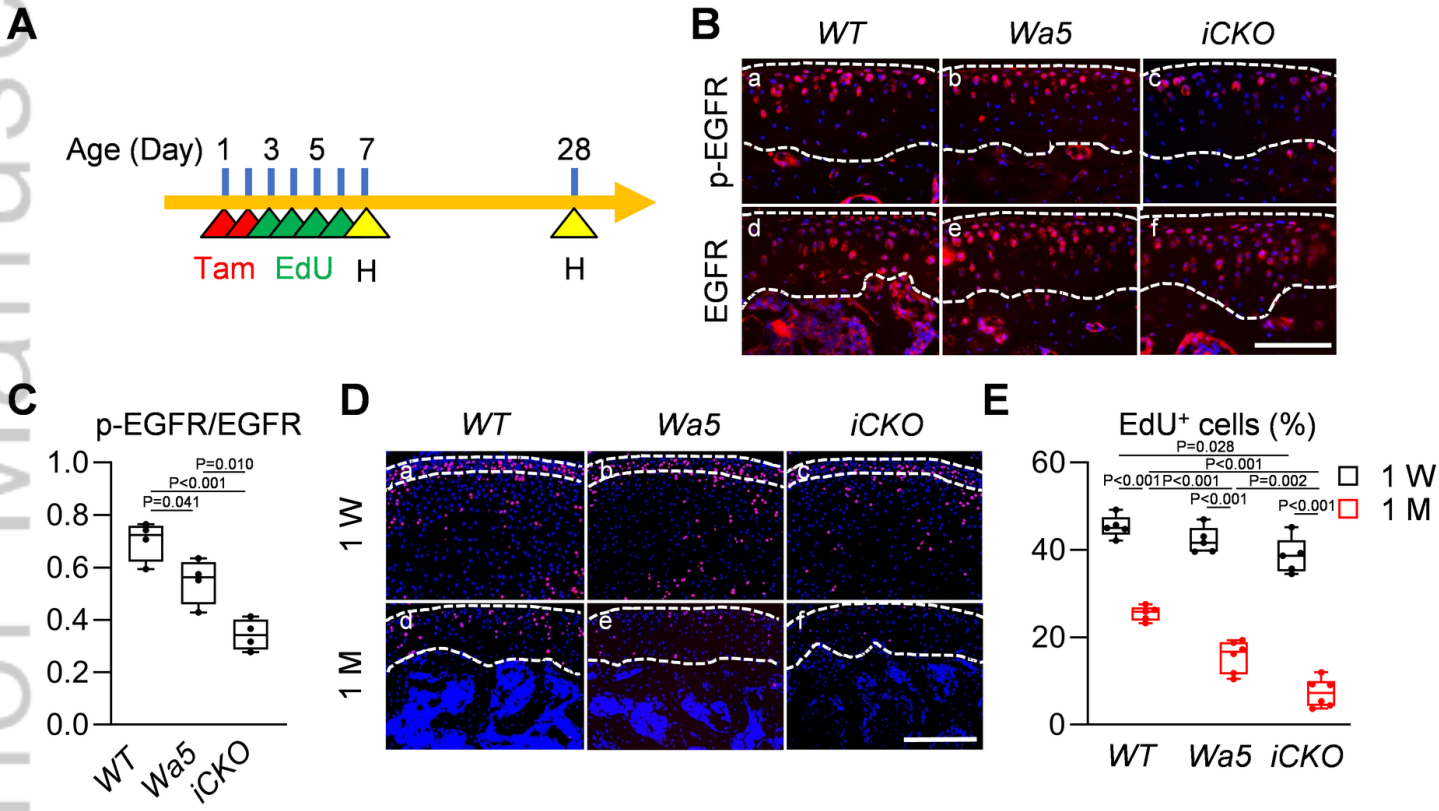

JBMR_4531_Figure 3.tif

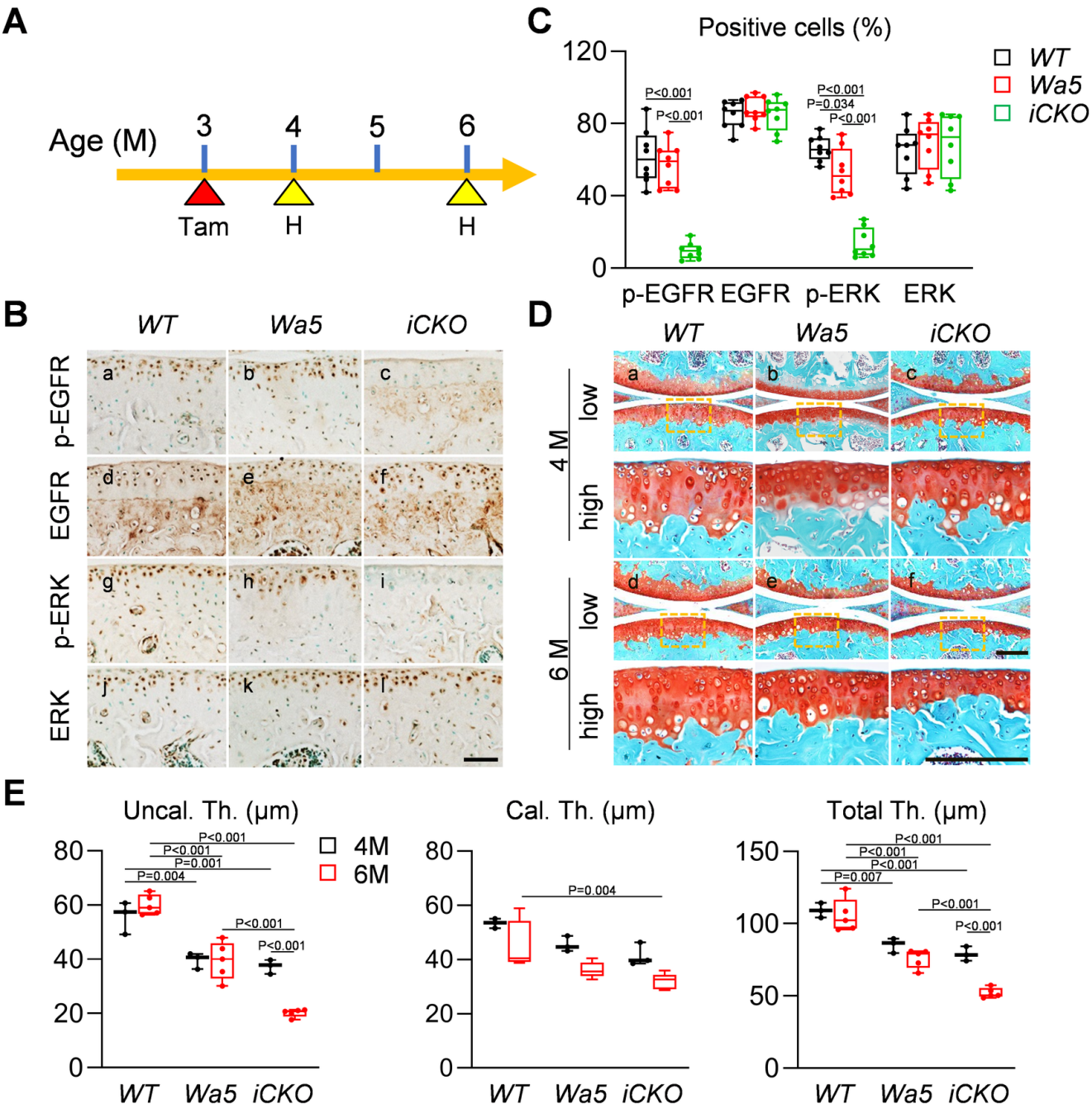

JBMR_4531_Figure 4.tif

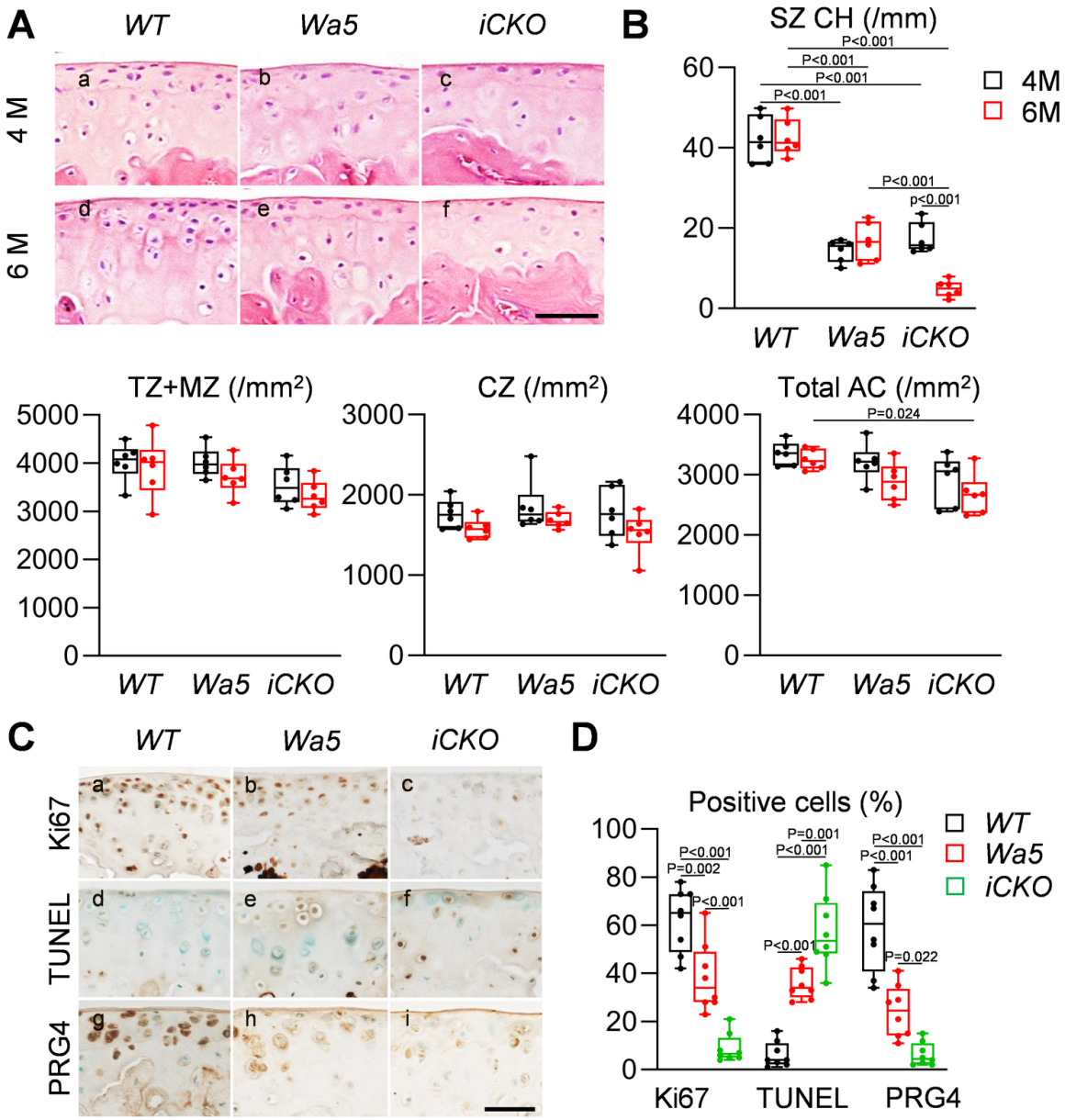

JBMR_4531_Figure 5.tif

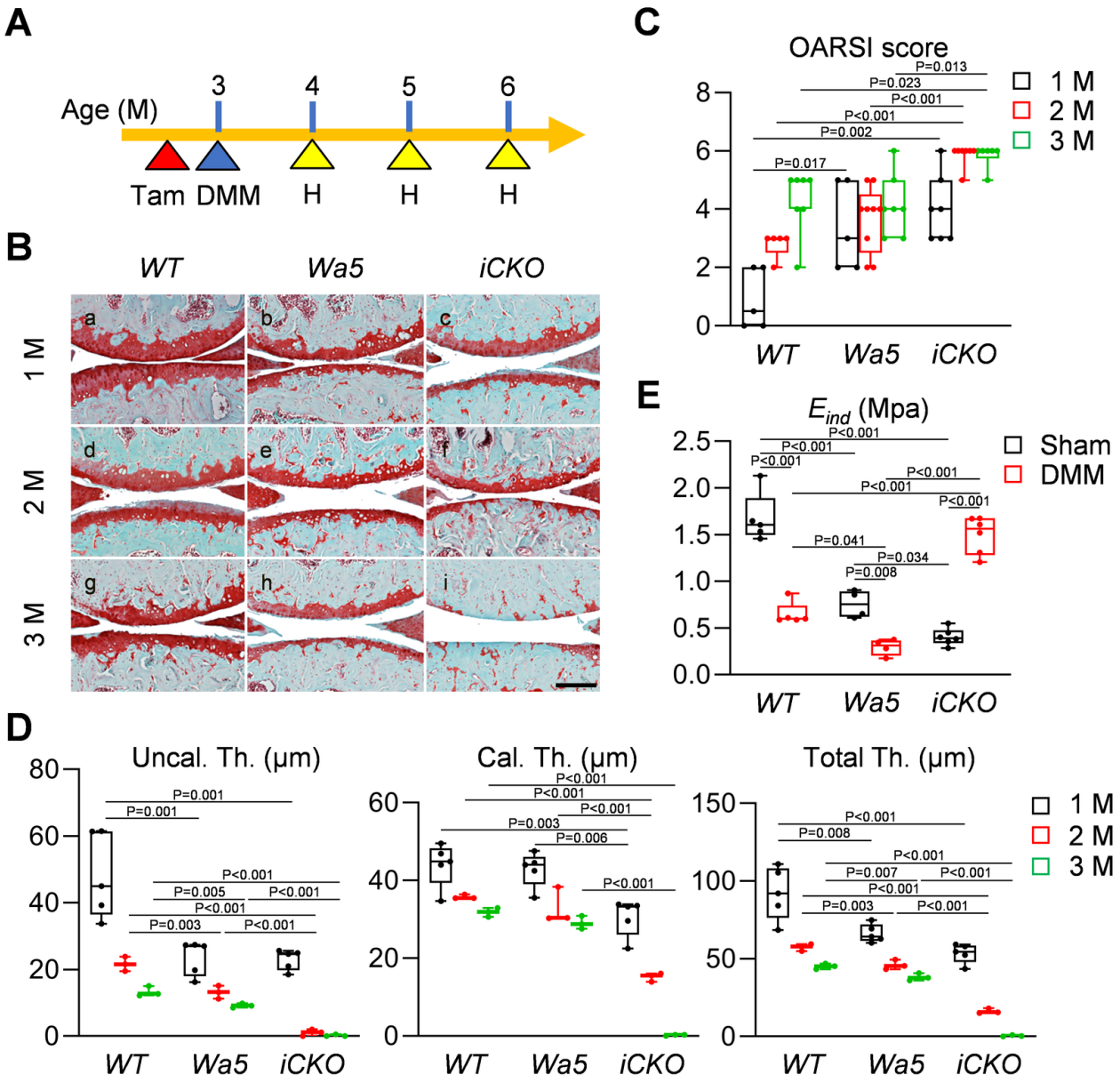

JBMR_4531_Figure 6.tif

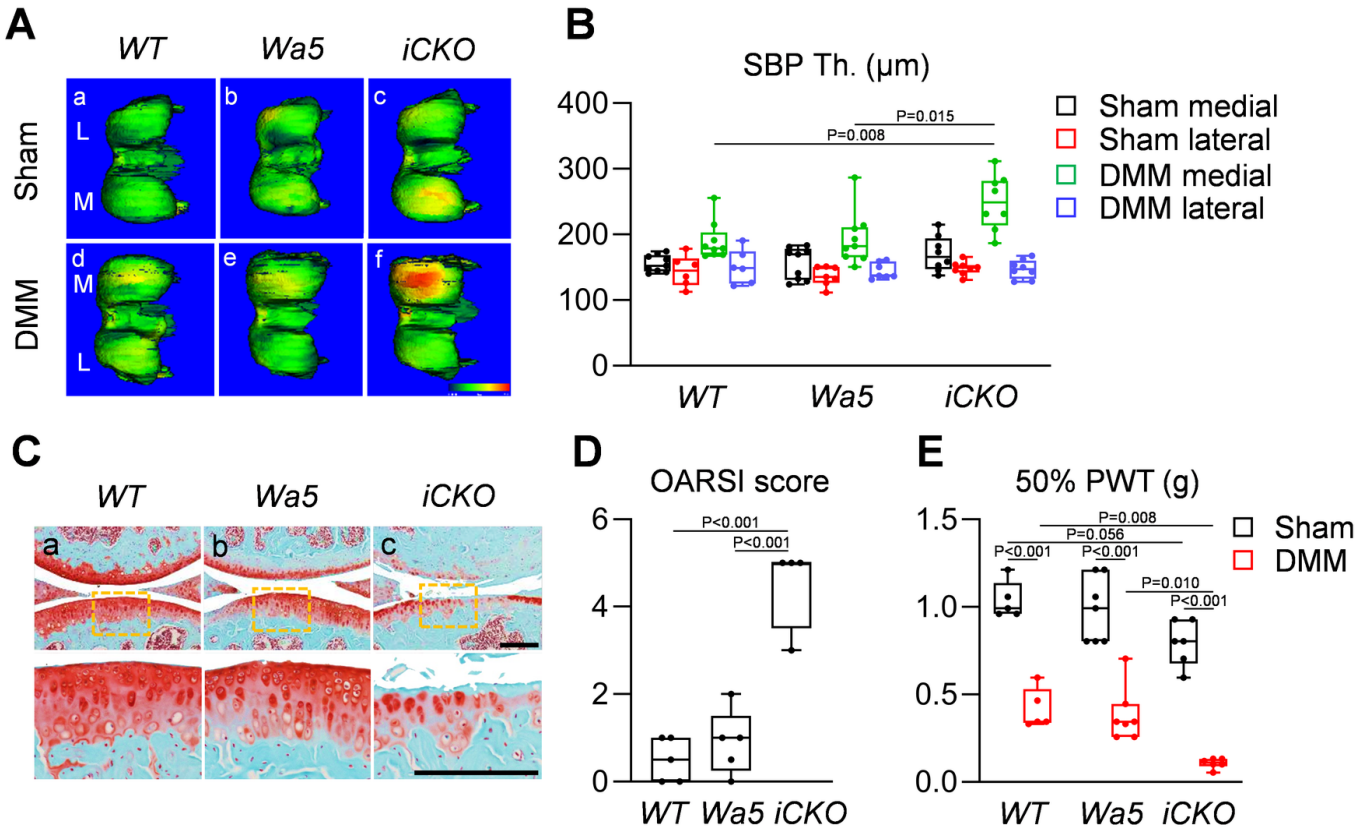

JBMR_4531_Figure 7.tif

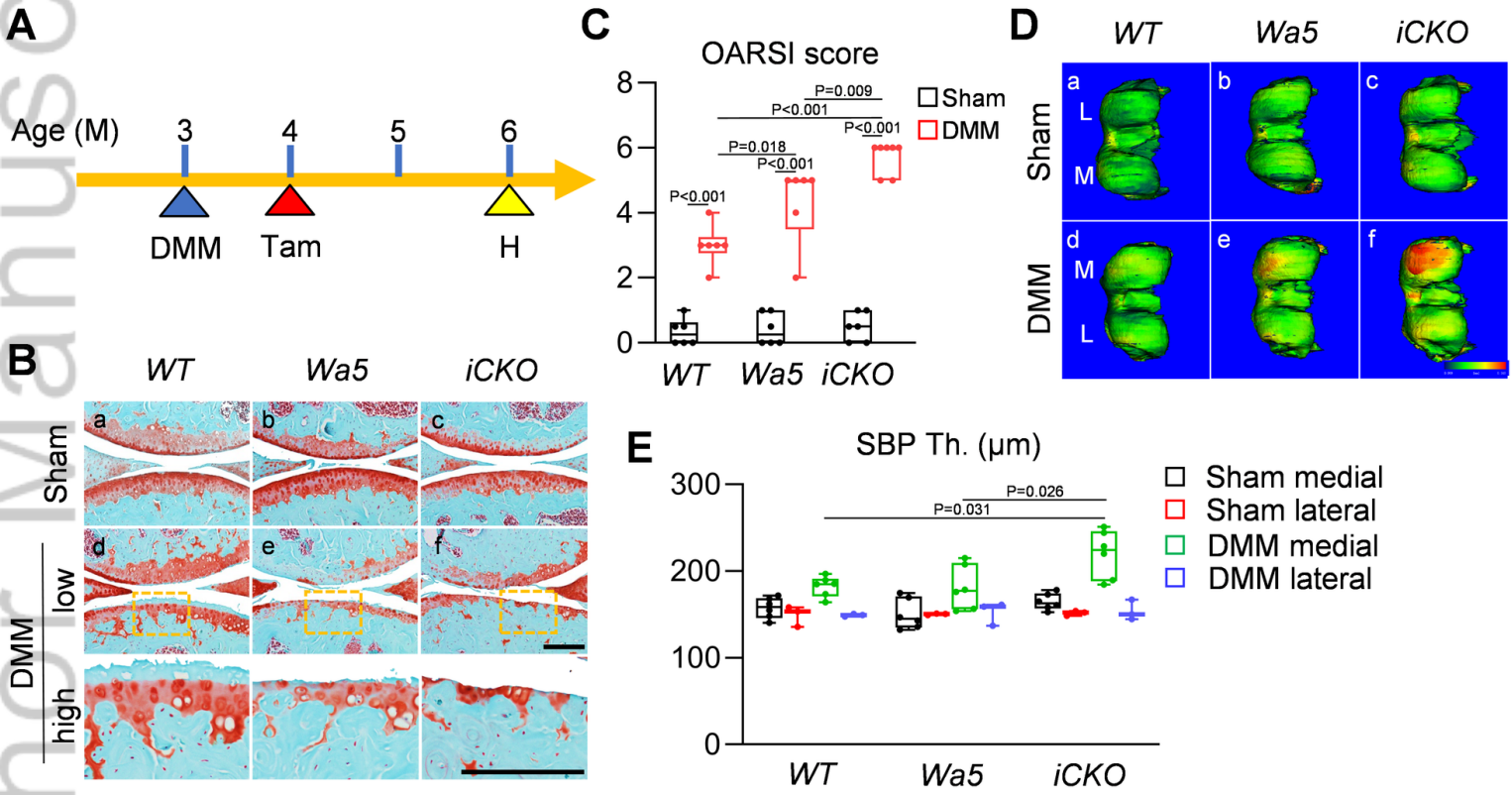

JBMR_4531_Figure 8.tif

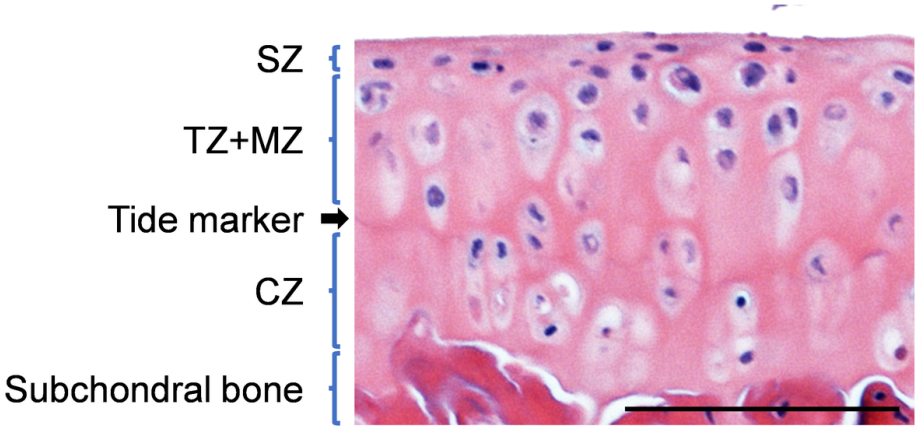

JBMR_4531_Figure S1.tif

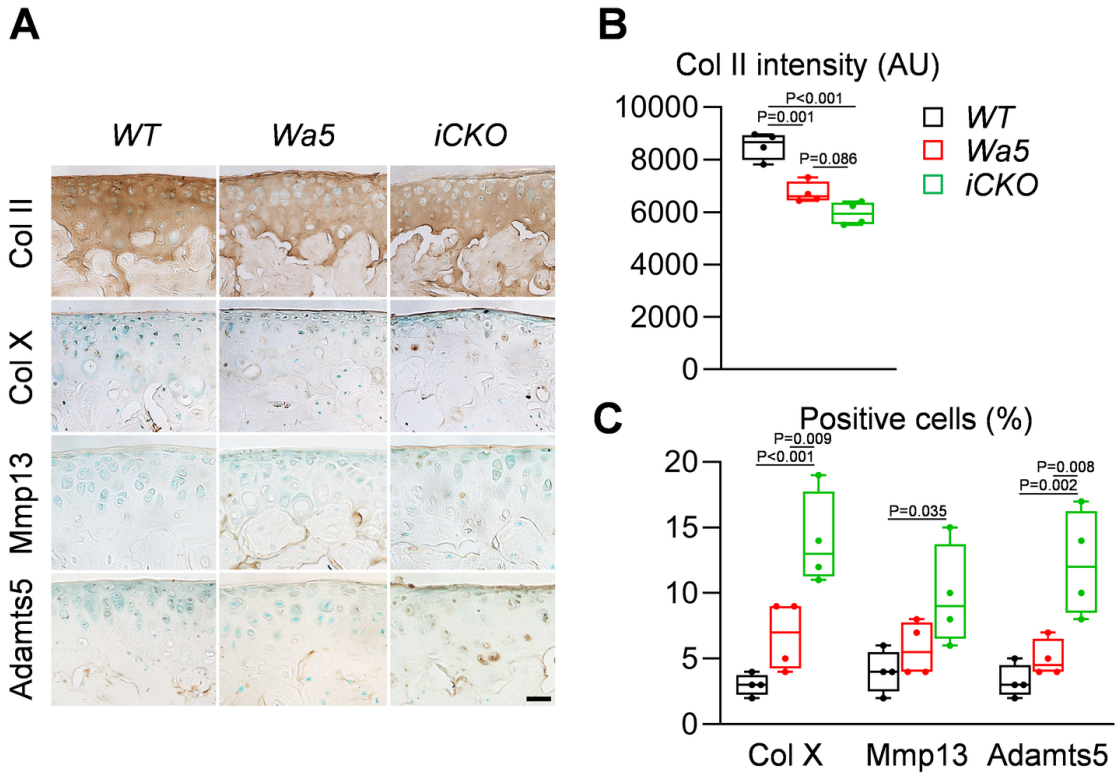

JBMR_4531_Figure S2.tif

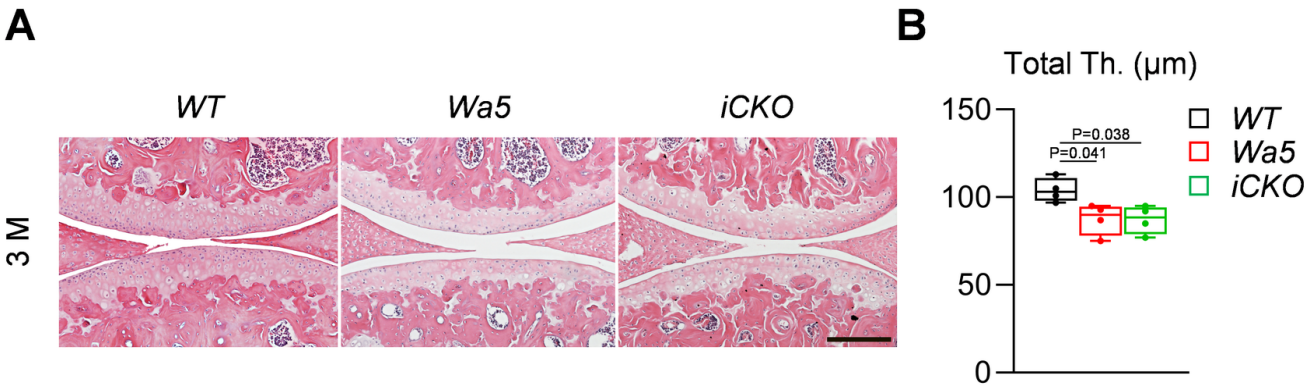

JBMR_4531_Figure S3.tif

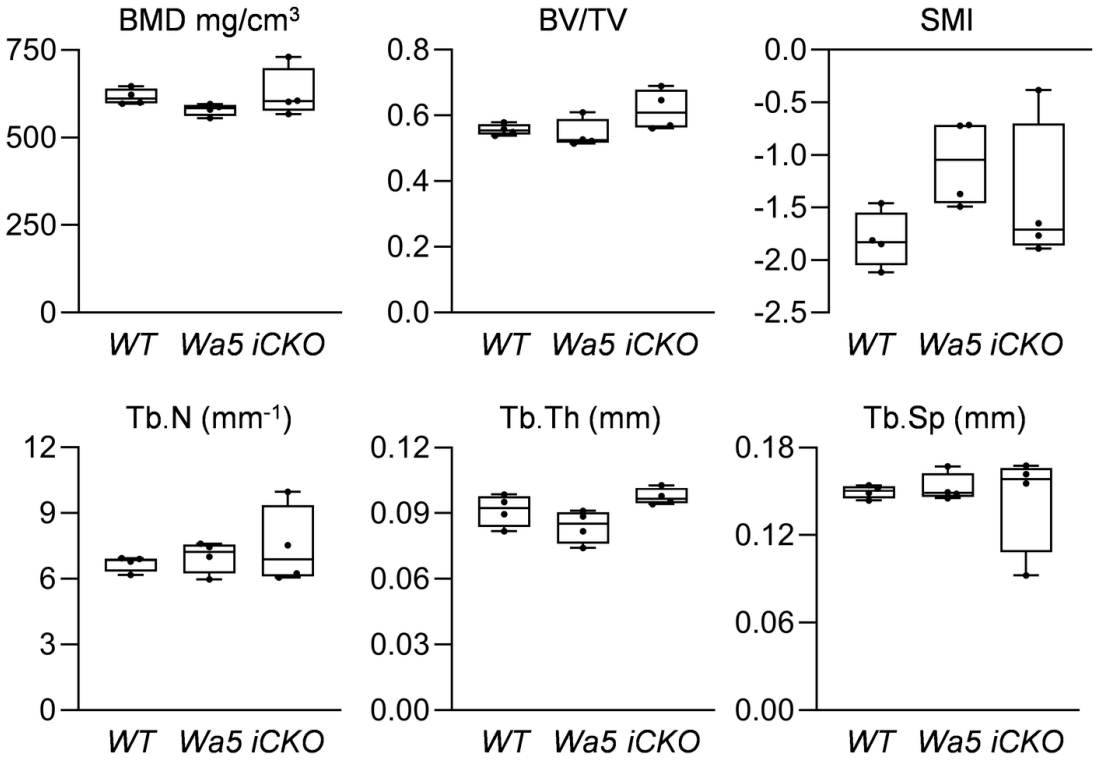

JBMR_4531_Figure S4.tif

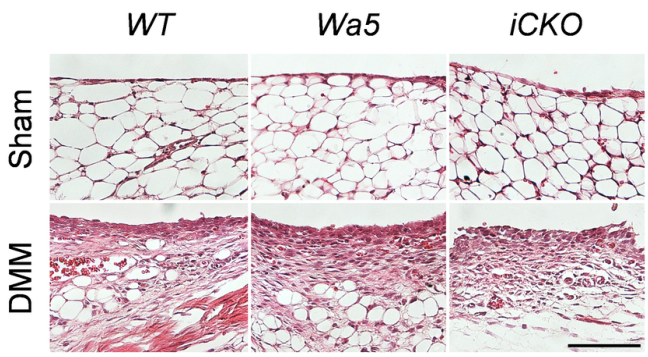

JBMR_4531_Figure S5.tif

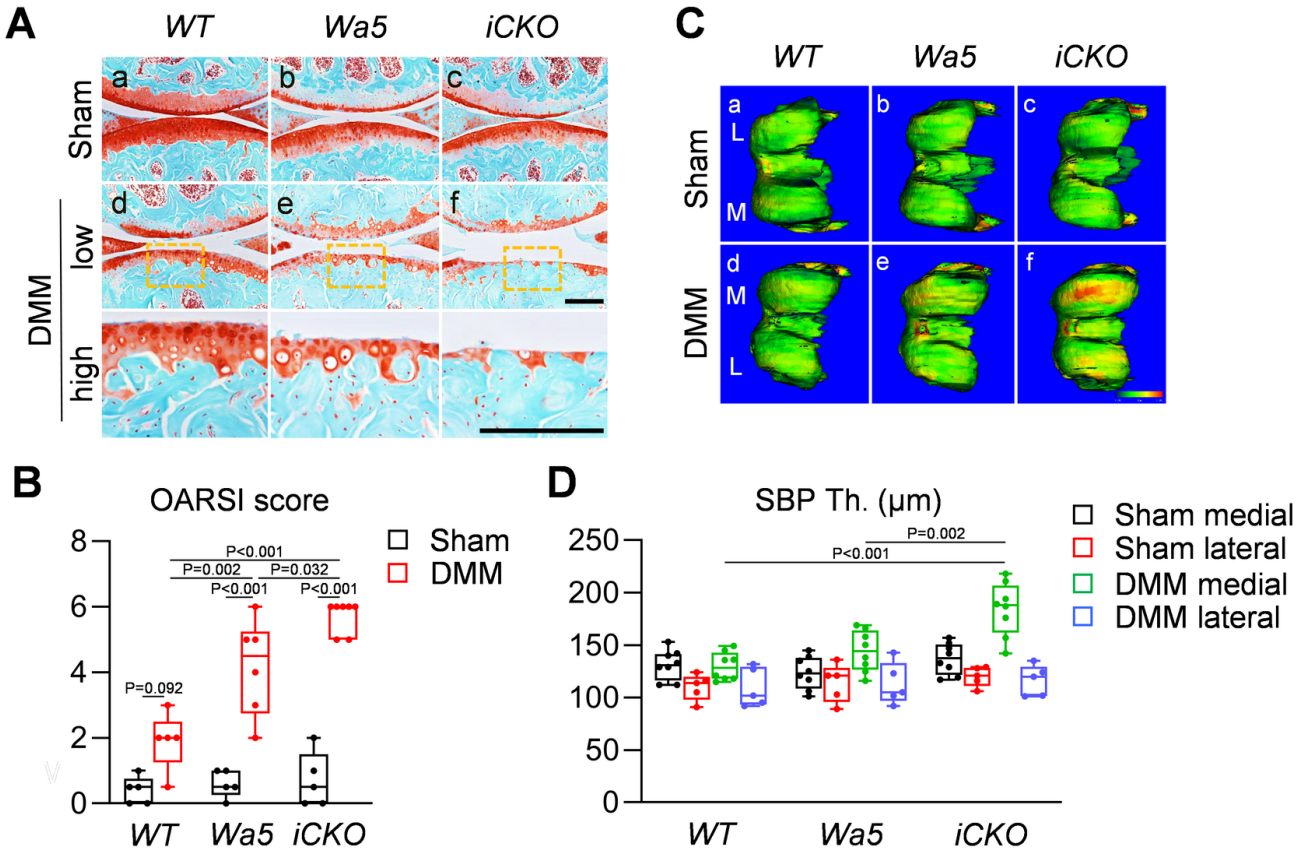

JBMR_4531_Figure S6.tif